JOURNAL OF COMPUTATIONAL PHYSICS 115, 86–106 (1994)

Investigation of Charged Particle Beam Stability: Numerical Method and Physical Results

VLADIMIR G. LEYMAN

Department of General Physics, Moscow Institute of Physics and Technology, Moscow, Russia

AND

SVETLANA P. LITVINTSEVA AND IGOR D. RODIONOV

Institute of Mathematical Modeling, Russian Academy of Sciences, Moscow 125047, Russia

Received January 7, 1994

Experiments on generation and transport of high current electron beams in gases and plasmas excite interest in studying their stability, which is reduced to solving a spectral boundary value problem for an ordinary second-order differential equation for some equilibrium beam configuration. The numerical technique which best satisfies the objectives of studying the beam stability and specific mathematical features of the correspondent spectral problem is the method of parameter evolution (MPE). In this paper a general scheme of the MPE is given, the evolution operator is derived for problems with smooth coefficients and the numerical algorithm is discussed. The problem of the bifurcations arising in the space of physical parameters is considered. An algorithm for predicting the point of bifurcation of a finite order and two algorithms for evolution across such a point are proposed. The following configurations of charged particle beams are studied on stability: a nonvortex tube electron beam in a longitudinal homogeneous magnetic field and radial electric field; and an isorotational vortex charged particle beam without the drift approximation.

0. INTRODUCTION

Experiments on generation and transport of high current electron beams in gases and plasmas excited interest in studying their stability. The results may also prove useful in various fields such as the generation of microwaves, controlled thermonuclear fusion, collective acceleration, powerful gas laser pumping, plasma–chemical reactor pumping, plasma heating by means of collective instabilities and others [1–3].

Generating electron beams of different configurations with given parameters is a separate problem of applied science—static electron optics [4]. The generation system consists of a set of external electric and magnetic fields including electrodes and conductors with currents required to generate electron beams of given configuration. We are interested mainly in propagation of the beam through a regular part of the generation system (the drift region), where the forces of space charge pushing electrons asunder and the effects of transverse electron velocities are compensated by focusing the forces of external electric and magnetic fields.

Dynamically equilibrium configurations of electron beams are not in thermodynamic equilibrium. There are two sources of such nonequilibrium: (1) potential energy concentrated in the proper Coulomb and magnetic fields of the beam and (2) kinetic energy corresponding to the field of a relative hydrodynamic beam velocity as a spatially inhomogeneous flow [5].

It is known that thermodynamically nonequilibrium states of dynamic equilibrium may prove to be unstable [6–7]. Development of instabilities in the beam results in violating its propagation or in its utter destruction, which is undesirable in many practical applications. In this connection the study of stationary electron beam stability is necessary.

Instability due to the two above causes of thermodynamic nonequilibrium may be referred to a class of hydrodynamic instabilities. The hydrodynamic (macroscopic) description of charged particle beams is based on moments of the Vlasov kinetic equation (the continuity and motion equations) and the Maxwell equations [8]. The equilibrium beam state may be found by solving a system of stationary equations for a beam of specific configuration.

An analysis of stability of equilibrium states against small perturbations is carried out in the framework of linear theory in the following way. Hydrodynamic variables and macroscopic fields are presented as a sum of their equilibrium values and perturbations. Linearizing the nonstationary equations near the equilibrium solution yields a

0021-9991/94 $6.00

system of equations describing the evolution of the perturbations. If the latter grow in time or space the equilibrium is unstable.

Studying the stability of the equilibrium beam configuration is usually reduced to solving a spectral boundary value problem for a system of differential equations. Many electron beams of practical interest possess a certain symmetry, for example, tape beams are plane-symmetrical while cylindrical beams are axisymmetric. For equilibrium configurations we may reduce the electron motion in such beams to a single dimension by a proper choice of the reference system. In this case a corresponding spectral boundary value problem is reduced to solving the ordinary second-order differential equation

$$\frac{d^2u(r)}{dr^2} + A(\lambda, \alpha, r)\frac{du(r)}{dr} + B(\lambda, \alpha, r)\cdot u(r) = 0,$$

$$\frac{1}{u(r)}\cdot\frac{du(r)}{dr}\bigg|_{r=0} = \Gamma_0(\lambda, \alpha), \qquad (0.1)$$

$$\frac{1}{u(r)}\cdot\frac{du(r)}{dr}\bigg|_{r=1} = \Gamma_1(\lambda, \alpha),$$

where $r \in [0;1]$ is the real spatial variable; $\alpha \in R$ is the real problem parameter ($\alpha \in R^n$ is a set of real parameters); $\lambda \in C$ is the complex eigenvalue; $u(r) \in W_2^1[0;1]$ is the complex-valued eigenfunction satisfying $\int_0^1 |u(r)|^2\,dr < \infty$ and $\int_0^1 |u'(r)|^2\,dr < \infty$; A, B, Γ_0, Γ_1 are continuously differentiated functions of their arguments.

The spectral parameter λ describes the beam stability against small perturbations in the form $A\cdot\exp\{i\lambda t\}$. If λ takes real values in the space of physical parameters determining the beam geometry, external focusing fields, the kind of perturbation, etc., the equilibrium under investigation is stable. If in a certain range of parameters λ takes complex values, then the equilibrium is unstable and $\delta = |\mathrm{Im}\,\lambda|$ is an increment of instability.

It is known that spectral boundary value problems of the form (0.1) are solved analytically very rarely. Therefore, a necessity arises in developing numerical techniques for their solution.

Now a great variety of methods for solving spectral problems are available. They may be divided into four large categories [9]: shooting methods, difference methods, methods of continuation, and approximation methods. However, the problems arising in studying the hydrodynamic stability of charged particle beams pose high demands on the efficiency of numerical codes.

The main objectives of studying the stability of beams are:

— to find regions of stability and instability in the space of physical parameters;

— to determine what perturbations have maximal increments and thus are most dangerous;

— to obtain dependences of maximal increment on beam geometry and other parameters;

— to work out practical recommendations on choosing optimal stable configurations, conditions for the beam input and confinement.

According to these objectives the spectral boundary value problems of the form (0.1) are solved for the entire range of parameter α variation rather than for its fixed value; i.e., the evolution curves $\lambda(\alpha)$ are calculated.

In addition, the problems of the form (0.1) have some specific mathematical features that impose stringent requirements on the choice of numerical technique:

1. The spectral boundary value problem (0.1) is not self-conjugate; i.e., the eigenvalue λ is complex while the eigenfunction $u(r)$ is complex-valued; therefore the methods oriented to solving self-conjugate problems cannot be used for solving (0.1). When using shooting methods the hit problem arises in the complex plane, which makes the calculations more difficult.

2. The eigenvalue λ is contained in the nonlinear form in the coefficients and boundary conditions. As a rule, nonlinear problems are solved by iterational methods. To calculate the evolution curve $\lambda(\alpha)$ it is necessary to solve a great number of problems of the same type. Using iterational methods results in longer computational times; therefore noniterational algorithms should be employed.

3. The problems are many-parametric; i.e., by α we mean a set of physical parameters $\{\alpha_1, ..., \alpha_n\}$. Thus, it is necessary to calculate a set of evolution curves $\{\lambda(\alpha_i)\}_{i=1}^n$ instead of only one $\lambda(\alpha)$. Hence, numerical methods oriented for solving only one problem are of low efficiency.

4. In the space of parameters there are bifurcations of the spectrum determined by physics of the phenomenon under investigation. Consequently on the evolution curve $\lambda(\alpha)$ the bifurcation points α^* may appear such that λ will take on real values when $\alpha < \alpha^*$ (i.e., the beam will be stable), and λ will have a complex value when $\alpha > \alpha^*$ (i.e., the beam will be unstable) or vice versa. Thus it is necessary to investigate the bifurcation points using the chosen numerical method. The numerical technique which best satisfies most of the above requirements is the method of parameter evolution (MPE) [10–12].

In Section I a general scheme of the MPE is given, the theorem about convergence of the MPE is proved, the evolution operator is derived for a problem with smooth coefficients, and the numerical algorithm is discussed. The problem of the bifurcations arising in the space of physical parameters is considered in Section II. An algorithm for predicting the points of bifurcation of finite order and two algorithms for evolution across the points of bifurcation of finite order are proposed.

In Section III problems of charged particle beam stability are studied by the method of parameter evolution. The stability of a nonvortex tube electron beam in a longitudinal homogeneous magnetic field and a radial electric field is studied in Section 3.1. For the first time the stability of an isorotational vortex charged particle beam has been studied *without the drift approximation in Section 3.2.*

I. METHOD OF PARAMETER EVOLUTION FOR NON-SELF-CONJUGATE SPECTRAL BOUNDARY VALUE PROBLEMS

1.1. A General Scheme of the Method

Spectral boundary value problems of the form (0.1), arising when the hydrodynamic stability of charged particle beams is analysed, are a particular case of stationary problems in mathematical physics. In terms of functional analysis they may be formulated in the form

$$F(x, \alpha) = 0, \tag{1.1}$$

where F: $X \times [0; 1] \Rightarrow Y$ is a nonlinear operator, X and Y are the Banach spaces, $x \in X$ is the desired solution (for example, in the problems of the form (0, 1) $x = \{\lambda, u(r)\}$), $\alpha \in [0; 1]$ is the problem parameter.

As noted above, studying the solution x depending on the parameter α over a whole range of its variation, i.e., constructing the evolution curve $x(\alpha)$, is of practical interest.

On the one hand, it is necessary to carry out many-variant calculations which requires high-efficiency algorithms. On the other hand, solving a set of problems, which are somewhat close in formulation, allows an enhancement in the efficiency by using results obtained earlier. Numerical methods based on such an approach are called continuation methods [13].

At the present time the continuation methods have been developed by using two approaches. The first approach, called parameter discretization, implies that after introducing a grid in parameter $\alpha: 0 = \alpha_0 < \alpha_1 < \cdots < \alpha_N = 1$ the equation $F(x, \alpha_{i+1}) = 0$ is solved by means of an iterational technique. An initial approximation at the point α_{i+1} is obtained by extrapolating solutions from α_i, $\alpha_{i-1}, \ldots$ (Fig. 1a). Taking $x^0_{i+1} = x_i$ as an initial approximation we may correct the solution by using the Newton method:

$$x^{s+1} = x^s - \left(\frac{\partial F(x^s, \alpha_{i+1})}{\partial x}\right)^{-1} \cdot F(x^s, \alpha_{i+1}). \tag{1.2}$$

The solution convergence for known conditions on F is provided by continuity of $x(\alpha)$ and hitting x^0 into the convergence region of Newtonian iterations [14].

The other approach, called the method of differentiation with respect to parameter or the method of parameter variation, is used when the operator $\partial F(x, \alpha)/\partial x$ is not degenerated in a vicinity of solution $x(\alpha)$. By differentiating (1.1) in parameter α we obtain the relation

$$\frac{dx}{d\alpha} = -\left(\frac{\partial F(x, \alpha)}{\partial x}\right)^{-1} \cdot \frac{\partial F(x, \alpha)}{\partial \alpha}, \tag{1.3}$$

which in the literature is sometimes called the Davidenko equation. Integration of (1.3) by the Euler scheme yields the scheme of continuation,

$$x_{i+1} = x_i - \left(\frac{\partial F(x_i, \alpha_i)}{\partial x}\right)^{-1} \cdot \frac{\partial F(x_i, \alpha_i)}{\partial \alpha} \cdot \delta\alpha_i, \tag{1.4}$$

where $x_i = x_i(\alpha_i)$, $\delta\alpha_i = \alpha_{i+1} - \alpha_i$ (Fig. 1b).

At the first approach, choosing the initial approximation $x^0_{i+1} = x_i$ and correcting the solution by the Newton method, we have the error to be equal to $O(\delta\alpha)$, which requires a smaller step in α to provide convergence of Newtonian iterations.

The accuracy of the scheme (1.4) is also $O(\delta\alpha)$. The main flaw of this scheme is the accumulation of errors in the evolution of the parameter α.

In [15] the scheme (1.4) was used to obtain the initial approximation at α_{i+1} and then the Newton scheme (1.2) was used to make the solution more precise (the combined scheme). Under such an approach an initial error in evalua-

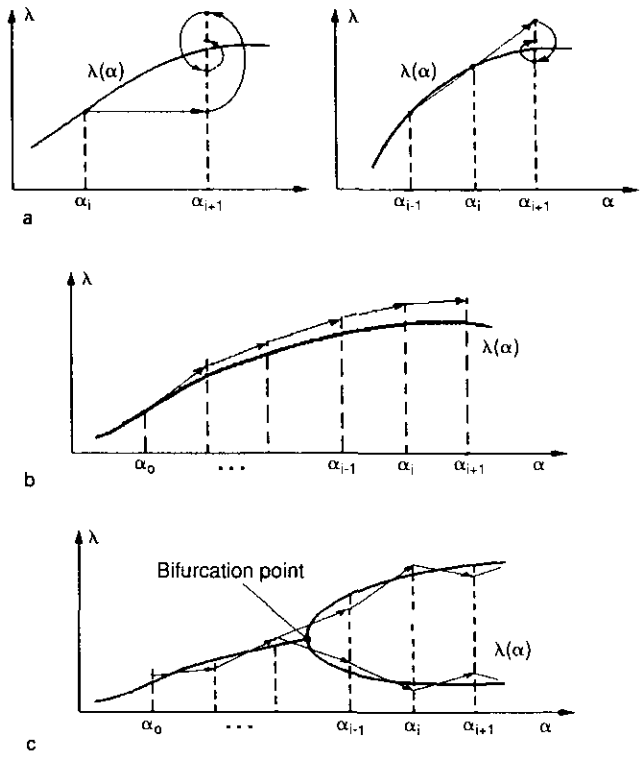

FIG. 1. Continuation methods: (a) Iterational methods; (b) Method of differentiation with respect to parameter; (c) Method of parameter evolution.

tion of x^0_{i+1} is $O(\delta\alpha^2)$, however, it requires at least twice the computation of $(\partial F(x, \alpha)/\partial x)^{-1}$ for each α_{i+1}.

In general, evaluating $(\partial F(x, \alpha)/\partial x)^{-1}$ requires long computational times; so the necessity of its multiple computation considerably reduces the efficiency of the numerical algorithm. Besides, the operator $\partial F(x, \alpha)/\partial x$ may prove to be degenerate at (x^*, α^*), which corresponds to the bifurcation point on the evolution curve $x(\alpha)$. In this case we cannot use the scheme (1.4). Special algorithms need to be developed for the evolution across the bifurcation points. Thus, the high efficiency of the continuation methods may only be achieved in a narrow class of problems.

One of the approaches that ensures such an efficiency is the MPE [16–17]. To construct the continuation scheme from point α_i to point α_{i+1} for its use in MPE, see (Fig. 1c), we should modify the problem (1.1) in the following way. Let x_i be its approximate solution, i.e., $F(x_i, \alpha_i) \neq 0$. On the interval $[\alpha_i, \alpha_{i+1}]$ we give the modified family of equations:

$$\tilde{F}(x, \alpha) = F(x, \alpha) - F(x_i, \alpha_i) \cdot \frac{\alpha - \alpha_{i+1}}{\alpha_i - \alpha_{i+1}}, \quad \alpha \in [\alpha_i, \alpha_{i+1}]. \tag{1.5}$$

This family satisfies the following relations:

$$\tilde{F}(x_i, \alpha_i) = 0, \quad \tilde{F}(x, \alpha_{i+1}) = F(x, \alpha_{i+1}). \tag{1.6}$$

By differentiating (1.5) with respect to α, we obtain the scheme of continuation,

$$x_{i+1} = x_i + L(x_i, \alpha_i) \cdot \delta\alpha_i + O(\delta\alpha^2), \tag{1.7}$$

on the interval $[\alpha_i, \alpha_{i+1}]$, where $L(x_i, \alpha_i)$ is the operator of evolution (OE) defined by

$$L(x_i, \alpha_i) = -\left[\frac{\partial F_i}{\partial x}\right]^{-1} \cdot \left\{\frac{\partial F_i}{\partial x} + \frac{F_i}{\delta\alpha_i}\right\}, \tag{1.8}$$

where $F_i = F(x_i, \alpha_i)$.

When computing the OE we simultaneously determine the correction

$$\delta x_i = -\left[\frac{\partial F_i}{\partial x}\right]^{-1} \cdot F_i,$$

wasting no additional computational time. This correction allows the determination of the solution for x_i more precisely at the point α_i by using the Newton method

$$\tilde{x}_i = x_i + \delta x_i + O(\delta\alpha^4).$$

Essentially the scheme (1.7)–(1.8) is the Euler scheme for differential equation (1.3) with the modified function $\tilde{F}(x, \alpha)$ of the form (1.5). As a consequence of (1.6) integration of this equation by the Euler scheme begins without an initial error. The accuracy of the value x_{i+1} obtained is determined by the accuracy of the Euler method at the single integrating step and is equal to $O(\delta\alpha^2)$. This fact is strictly proved below.

Thus the continuation scheme in the MPE has a higher order of accuracy than the scheme used in the parameter discretization method and than the scheme used in the method of parameter variation. As compared with the combined scheme, the scheme (1.7)–(1.8) has the same order of accuracy, but it requires calculating $[\partial F/\partial x]^{-1}$ only once per point of grid in α; i.e., this scheme is more economical. Such efficiency is achieved by combination of the parameter evolution (the term $-(\partial F_i/\partial x)^{-1} \cdot (\partial F_i/\partial\alpha) \cdot \delta\alpha_i$ in the MPE continuation scheme (1.7)–(1.8)) with the Newton correction (the term $-(\partial F_i/\partial x)^{-1} \cdot F_i$).

The convergence conditions of the difference solution (1.7) to exact one are analogous to the conditions of known theorems about the implicit function and about the convergence of the Newton method. They are determined by the following theorem.

THEOREM (About convergence of the MPE). *Let $x(\alpha)$ be a solution of a functional equation*

$$F(x(\alpha), \alpha) = 0,$$

where $\alpha \in [0; 1]$, $x \in X$, $F: X \times [0; 1] \Rightarrow Y$ is a Fréchet differentiated nonlinear operator, X and Y are the Banach spaces. Let $\Omega_\alpha = \{x: \|x - x(\alpha)\| \leqslant a\}$ be the neighborhood of the $x(\alpha)$ solution. Assume that the following conditions are satisfied:

(1) $\|F'_x(x, \alpha)^{-1}\| \leqslant a_1$, $\forall x \in \Omega_a$;

(2) $\|F(x_1, \alpha_1) - F(x_2, \alpha_2) - F'_x(x_2, \alpha_2)(x_1 - x_2) - F'_\alpha(x_2, \alpha_2)(\alpha_1 - \alpha_2)\| \leqslant a_2 \|x_1 - x_2\|^2 + a_3 |\alpha_1 - \alpha_2|^2$, $\forall x_1, x_2 \in \Omega_a$, $\forall \alpha_1, \alpha_2 \in [0; 1]$;

(3) $\|\{F'_\alpha(x, \alpha)\}^{-1}\| \leqslant a_4$, $\forall x \in \Omega_a$;

(4) $\tilde{x}_0 \in \Omega_a$, *where $\tilde{x}_0$ is an initial value of desired numerical solution assigned with a some error.*

Then there exists such a value of a that for any fixed $\alpha \in [0; 1]$ the difference solution (1.7) would converge to a precise one for $\delta\alpha \to 0$, i.e., $x_N \to x(\alpha)$ for $N \to \infty$, where $\delta\alpha = \alpha/N$, $\alpha_i = i \cdot \delta\alpha$, $i = 1, 2, ..., N$. The convergence rate estimate is valid:

$$\|x_N - x(\alpha)\| \leqslant \tilde{A} \cdot |\delta\alpha|^2 + g_N, \tag{1.9}$$

where $0 \leqslant g_N \leqslant (B\varepsilon_0)^N \varepsilon_0$, $\varepsilon_0 = \|\tilde{x}_0 - x(0)\| + D|\delta\alpha|$, while $0 \leqslant g_N \leqslant (1/B) \cdot (B\varepsilon_0)^{2^N}$ for $\delta\alpha = 0$; $\tilde{A}$, B, D are constants.

Proof. Expression (1.7) provides

$$(x_{i+1}-x_i)\cdot\frac{\partial F_i}{\partial x}+\delta\alpha\cdot\frac{\partial F_i}{\partial\alpha}=-F_i. \tag{1.10}$$

From condition (2), taking $\alpha_1=\alpha_{i+1}$, $\alpha_2=\alpha_i$, $x_1=x(\alpha_{i+1})$, $x_2=x_i$, we have

$$(x(\alpha_{i+1})-x_i)\cdot\frac{\partial F_i}{\partial x}+\delta\alpha\cdot\frac{\partial F_i}{\partial\alpha}=-F_i+\varepsilon, \tag{1.11}$$

where

$$\|\varepsilon\|\leqslant a_2\,\|x(\alpha_{i+1})-x_i\|^2+a_3\,|\delta\alpha|^2. \tag{1.12}$$

Subtracting (1.10) from (1.11) and due to condition (1) and estimate (1.12) we have

$$\|x(\alpha_{i+1})-x_{i+1}\|\leqslant a_1a_2\cdot\|x(\alpha_{i+1})-x_i\|^2+a_1a_3\,|\delta\alpha|^2. \tag{1.13}$$

An inequality takes place:

$$\|x(\alpha_{i+1})-x_i\|\leqslant\|x(\alpha_{i+1})-x(\alpha_i)\|+\|x(\alpha_i)-x_i\|. \tag{1.14}$$

From Equation (1.3) and conditions (1) and (3) of the theorem an estimate follows:

$$\|x(\alpha_{i+1})-x(\alpha_i)\|\leqslant a_1a_4\,|\delta\alpha|. \tag{1.15}$$

Considering (1.14) and (1.15) the inequality (1.13) may be written as

$$\|x(\alpha_{i+1})-x_{i+1}\|\leqslant a_1a_2\cdot\{a_1a_4\,|\delta\alpha|+\|x(\alpha_i)-x_i\|\}^2+a_1a_3\,|\delta\alpha|^2. \tag{1.16}$$

For $\delta\alpha\to 0$ we have

$$\|x(\alpha_{i+1})-x_{i+1}\|\leqslant B\cdot\|x(\alpha_i)-x_i\|^2,\qquad\text{where}\quad B=a_1a_2.$$

Therefrom it follows that

$$\|x_N-x(\alpha)\|\leqslant\frac{1}{B}\cdot(B\cdot\|\tilde{x}_0-x(0)\|)^{2^N}. \tag{1.17}$$

Then we may take in such $a<1/a_1a_2$ that

$$B\cdot\|\tilde{x}_0-x(0)\|\leqslant B\cdot a<1. \tag{1.18}$$

Convergence of $x_N\to x(\alpha)$ for $\delta\alpha\to 0$ follows from (1.17)–(1.18).

The convergence rate estimate comes from (1.16). Denoting $\Delta_i=\|x_i-x(\alpha_i)\|$, $A=a_1a_3$, $D=a_1a_4$, the inequality (1.16) is rewritten as

$$\Delta_{i+1}\leqslant B\cdot(D\,|\delta\alpha|+\Delta_i)^2+A\cdot|\delta\alpha|^2. \tag{1.19}$$

Let us find such $\Delta_{\max}$ that for $\Delta_i>\Delta_{\max}$ the process would diverge. It should satisfy the conditions $\Delta_{i+1}=\Delta_i=\Delta_{\max}$ and the equation in the expression (1.19):

$$\Delta_{\max}=\frac{1}{2B}\cdot(1-2BD\,|\delta\alpha|+\sqrt{1-4B\,|\delta\alpha|\cdot(D+A\,|\delta\alpha|)})\leqslant\frac{1}{B}.$$

We introduce the notation $\varepsilon_i=\Delta_i+D\,|\delta\alpha|$; then (1.19) is rewritten as

$$\varepsilon_{i+1}\leqslant B\varepsilon_i^2+C, \tag{1.20}$$

where $C=A\,|\delta\alpha|^2+D\,|\delta\alpha|$. From (1.20) it follows that

$$\begin{aligned}&\varepsilon_{i+1}\leqslant(B\varepsilon_{\max})\,\varepsilon_i+C=\tilde{B}\varepsilon_i+C,\\&\varepsilon_{\max}=\Delta_{\max}+D\,|\delta\alpha|.\end{aligned} \tag{1.21}$$

Then the estimate for ε_N will be

$$\varepsilon_N\leqslant\tilde{B}^N\varepsilon_0+(\tilde{B}^{N-1}+\tilde{B}^{N-2}+\cdots+1)\cdot C.$$

Therefore substituting the expressions for ε_N and C and using the definition of $\Delta_{\max}$ we have

$$\Delta_N\leqslant(B\varepsilon_0)^N\,\varepsilon_0+A\,|\delta\alpha|^2+\tilde{B}C\cdot\frac{\tilde{B}^{N-2}-1}{\tilde{B}-1}. \tag{1.22}$$

(1.22) and (1.17) testify to the validity of (1.9) estimate of the initial data error relaxation rate.

Now we prove the second order of the method by $|\delta\alpha|$. To make it we show that we have an inequality,

$$\varepsilon_N\leqslant B^N\cdot\varepsilon_0^2\cdot P_{2^{(N-1)}-1}(\varepsilon_0^2)+BC^2\cdot\underbrace{(BC\cdot(BC\cdot\cdots\cdot(BC}_{(N-2)\text{ times}}+1)^2+1)^2+\cdots+1)^2}_{(N-2)\text{ times}}+C, \tag{1.23}$$

where $P_{2^{(N-1)}-1}(\varepsilon_0^2)$ is a polynomial of $(2^{(N-1)}-1)$ power respectively to (ε_0^2). We apply the induction technique for the proof. For $N=1$ we have

$$\varepsilon_1\leqslant B^1\cdot\varepsilon_0^2\cdot 1+C.$$

The inequality (1.23) is true, because 1 is the polynomial of zero power with respect to any variable, and the second term in (1.23) exists only for $N \geqslant 2$. For $N = 2$

$$\varepsilon_2 \leqslant B\varepsilon_1^2 + C \leqslant B^2\varepsilon_0^2 \cdot (B\varepsilon_0^2 + 2C) + BC^2 + C;$$

i.e., (1.23) is also true. Let (1.23) be true for $N = k$. Prove its validity for either $N = k + 1$:

$$\begin{aligned}
\varepsilon_{k+1} &\leqslant B\varepsilon_k^2 + C \leqslant B \cdot \{B^k \cdot \varepsilon_0^2 \cdot P_{2^{(k-1)}-1}(\varepsilon_0^2) + BC^2 \\
&\cdot \underbrace{(BC \cdot (BC \cdot \cdots \cdot (BC}_{(k-2)\text{ times}} \underbrace{+ 1)^2 + 1)^2 + \cdots + 1)^2}_{(k-2)\text{ times}} \\
&+ C\}^2 + C; \\
\varepsilon_{k+1} &\leqslant B^{k+1}\varepsilon_0^2 \cdot \{B^k \cdot \varepsilon_0^2 \cdot P_{2^{(k-1)}-1}^2(\varepsilon_0^2) \\
&+ 2P_{2^{(k-1)}-1}(\varepsilon_0^2) \times (BC^2 \\
&\cdot \underbrace{(BC \cdot (BC \cdot \cdots \cdot (BC}_{(k-2)\text{ times}} \underbrace{+ 1)^2 + 1)^2 + \cdots + 1)^2}_{(k-2)\text{ times}} \\
&+ C)\} + BC^2 \\
&\cdot \underbrace{(BC \cdot (BC \cdot \cdots \cdot (BC}_{(k-1)\text{ times}} \underbrace{+ 1)^2 + 1)^2 + \cdots + 1)^2}_{(k-1)\text{ times}} \\
&+ C. \qquad (1.24)
\end{aligned}$$

Note that the polynomial $\varepsilon_0^2 \cdot P_{2^{(k-1)}-1}^2(\varepsilon_0^2)$ is the polynomial of power $2 \cdot (2^{k-1} - 1) + 1 = 2^k - 1$. So (1.24) is rewritten as

$$\begin{aligned}
\varepsilon_{k+1} &\leqslant B^{k+1}\varepsilon_0^2 \cdot P_{2^k-1}(\varepsilon_0^2) + BC^2 \\
&\cdot \underbrace{(BC \cdot (BC \cdot \cdots \cdot (BC}_{(k-1)\text{ times}} \underbrace{+ 1)^2 + 1)^2 + \cdots + 1)^2}_{(k-1)\text{ times}} \\
&+ C.
\end{aligned}$$

Thus the (1.23) inequality is proved. Substituting ε_N and C into (1.23) we have

$$\begin{aligned}
\Delta_N &\leqslant B^N \cdot \varepsilon_0^2 \cdot P_{2^{(N-1)}-1}(\varepsilon_0^2) + BC^2 \\
&\cdot \underbrace{(BC \cdot (BC \cdot \cdots \cdot (BC}_{(N-2)\text{ times}} \underbrace{+ 1)^2 + 1)^2 + \cdots + 1)^2}_{(N-2)\text{ times}} \\
&+ A\,|\delta\alpha|^2. \qquad (1.25)
\end{aligned}$$

The second term in the right side of (1.25) has the same smallness order of $|\delta\alpha|$ as C^2, and $C^2 \sim |\delta\alpha|^2$. The validity of the theorem is proved herein.

Hence, in the course of the evolution of the parameter α an accumulated error relaxes to a certain level determined by the size of the step in α. Thus within the framework of the MPE, we may automatically choose the step in α in order to provide an accuracy of the numerical solution not lower than desired.

1.2. Evolution Operator for Problems with Smooth Coefficients

The initial value problem

$$\begin{aligned}
&\frac{dx}{d\alpha} = L(x, \alpha), \qquad \alpha \in [0; 1], \\
&x(0) = x_0.
\end{aligned} \qquad (1.26)$$

will be called the evolution problem, where $L(x, \alpha)$ is the evolution operator. The problem (1.1) may be reduced to (1.26) in some methods of continuation. At the functional level the evolution operator in MPE has the form (1.8). Now we shall construct the OE for the spectral boundary value problem for ordinary differential equation, ODE, of the second order in the form (0.1).

Note that the problem (0.1) is nonlinear with respect to the eigenvector $x = \{\lambda, u(r)\}$ and the spectral parameter λ which nonlinearly enters into the coefficients $A(\lambda, \alpha, r)$ and $B(\lambda, \alpha, r)$, and into the boundary conditions $\Gamma_0(\lambda, \alpha)$ and $\Gamma_1(\lambda, \alpha)$. The problem under consideration is linear with respect to the eigenfunction $u(r)$. This means that if the eigenvalue λ is known then to calculate the eigenfunction $u(r)$ we should solve the linear boundary value problem. Economical algorithms for solving such problems are constructed based upon the back substitution method [18]. One of these algorithms is considered in Section 1.3 and used for calculating the eigenfunction $u(r)$.

Thus, it is expedient to reduce the problem in the form (0.1) to the evolution problem with respect to the spectral parameter λ rather than the whole eigenvector $x = \{\lambda, u(r)\}$ and thus reduce the dimension of the respective evolution problem [17].

By replacing the function $u(r)$ in (0.1) by

$$D(r) = \frac{1}{u(r)} \cdot \frac{du(r)}{dr} + \frac{1}{2} A(\lambda, \alpha, r), \qquad (1.27)$$

we pass to the problem

$$\begin{aligned}
&\frac{dD(r)}{dr} + D^2(r) + U(\lambda, \alpha, r) = 0. \\
&D(0) = \Gamma_0(\lambda, \alpha) + 0.5 \cdot A(\lambda, \alpha, 0), \\
&D(1) = \Gamma_1(\lambda, \alpha) + 0.5 \cdot A(\lambda, \alpha, 1),
\end{aligned} \qquad (1.28)$$

where

$$\begin{aligned}
U(\lambda, \alpha, r) = &-\frac{1}{2}\frac{d}{dr} A(\lambda, \alpha, r) \\
&-\frac{1}{4} \cdot A^2(\lambda, \alpha, r) + B(\lambda, \alpha, r). \qquad (1.29)
\end{aligned}$$

Let us also introduce the function $\psi(r)$ which is connected with $D(r)$ by the relation

$$\frac{1}{\psi(r)} \cdot \frac{d\psi(r)}{dr} = D(r). \tag{1.30}$$

By differentiating (1.28) with respect to the parameter α we obtain an equation with respect to $y(r) = dD(r)/d\alpha$,

$$\frac{dy(r)}{dr} + 2 \cdot D(r) \cdot y(r) + \frac{dU}{d\alpha}(\lambda, \alpha, r) = 0, \tag{1.31}$$

which has the solution

$$y(r) = \frac{\psi^2(0)}{\psi^2(r)} \cdot y(0) - \frac{1}{\psi^2(r)} \cdot \int_0^r \psi^2(r') \frac{dU}{d\alpha}(\lambda, \alpha, r')\, dr'. \tag{1.32}$$

From this, by involving the boundary conditions, we obtain the expression for the evolution operator,

$$\frac{d\lambda}{d\alpha} = L(\lambda, \alpha) = -\frac{L_\alpha(\lambda, \alpha)}{L_\lambda(\lambda, \alpha)}, \tag{1.33}$$

where

$$\begin{aligned} L_\gamma(\lambda, \alpha) = &\left\{\frac{\partial \Gamma_1}{\partial \gamma}(\lambda, \alpha) + \frac{1}{2}\frac{\partial A}{\partial \gamma}(\lambda, \alpha, 1)\right\} \cdot \psi^2(1) \\ &- \left\{\frac{\partial \Gamma_0}{\partial \gamma}(\lambda, \alpha) + \frac{1}{2} \cdot \frac{\partial A}{\partial \gamma}(\lambda, \alpha, 0)\right\} \cdot \psi^2(0) \\ &+ \int_0^1 \psi^2(r) \frac{\partial U}{\partial \gamma}(\lambda, \alpha, r)\, dr, \qquad \gamma \in \{\lambda, \alpha\}. \end{aligned} \tag{1.34}$$

Here substituting $\gamma = \alpha$ and $\partial/\partial\gamma = \partial/\partial\alpha$, we obtain the numerator $L_\alpha(\lambda, \alpha)$ of the OE. Analogously for $\gamma = \lambda$ and $\partial/\partial\gamma = \partial/\partial\lambda$ we obtain the denominator $L_\lambda(\lambda, \alpha)$ of the OE (1.33).

In accordance with Section 1.1 relaxation properties are introduced into OE (1.33)–(1.34) by means of Newton correction, the specific form of which is given in Section 1.3.

1.3. Numerical Algorithm

We consider the numerical algorithm for solving the spectral boundary value problem in the form (0.1) with smooth coefficients. For simplicity we write down (0.1) in the form

$$\begin{aligned} &\psi''(r) + U(\lambda, \alpha, r)\, \psi(r) = 0, \qquad r \in [0; 1], \\ &\psi'(0)/\psi(0) = \Phi_0(\lambda, \alpha), \\ &\psi'(1)/\psi(1) = \Phi_1(\lambda, \alpha), \end{aligned} \tag{1.35}$$

where the function $U(\lambda, \alpha, r)$ is connected with coefficients $A(\lambda, \alpha, r)$ and $(B(\lambda, \alpha, r)$ by the relation (1.29). The boundary conditions are

$$\Phi_0(\lambda, \alpha) = \Gamma_0(\lambda, \alpha) + 0.5 \cdot A(\lambda, \alpha, 0);$$
$$\Phi_1(\lambda, \alpha) = \Gamma_1(\lambda, \alpha) + 0.5 \cdot A(\lambda, \alpha, 1);$$

and $\psi(r)$ is the desired eigenfunction to within the multiplier in the form $C \cdot \exp\{0.5 \cdot \int_0^r A(\lambda, \alpha, r')\, dr'\}$, where C is an arbitrary constant.

If for the given α_i we know an approximate eigenvalue, λ_i, the problem (1.35) is linear with respect to $\psi(r)$. The back substitution method [19] is the most economical for computing the approximate eigenfunction. We consider a variant of this method [16].

Now we shall pass from the problem (1.35) to the problem with respect to the logarithmic derivative of eigenfunction $D(r) = \psi'(r)/\psi(r)$:

$$\begin{aligned} &D'(r) + D^2(r) + U(\lambda, \alpha, r) = 0 \\ &D(0) = \Phi_0(\lambda, \alpha) \\ &D(1) = \Phi_1(\lambda, \alpha). \end{aligned} \tag{1.36}$$

Let the function $D_L(r)$ be the solution of the Cauchy problem with the initial condition at point $r = 0$. Correspondingly, $D_R(r)$ is the solution of the Cauchy problem with the initial condition at $r = 1$. Since the eigenvalue λ_i is approximately known and there are errors of the difference approximation, we have $D_L(r) \neq D_R(r)$. It is clear that the eigenfunction $\psi(r)$ obtained by solving the equation

$$\psi'(r) - D(r) \cdot \psi(r) = 0 \tag{1.37}$$

will best satisfy (1.35) if we take

$$D(r) = \begin{cases} D_L(r), & 0 \leqslant r \leqslant r_s, \\ D_R(r), & r_s \leqslant r \leqslant 1, \end{cases} \tag{1.38}$$

where the solution joint point, r_s, is chosen from the condition

$$\begin{aligned} &|\Delta(r_s)| = \min_{(0;\,1)} |\Delta(r)| \\ &\Delta(r) = D_R(r) - D_L(r). \end{aligned} \tag{1.39}$$

The function $D(r)$ thus constructed satisfies (1.36) everywhere on $[0; 1]$ except at the joint point, r_s. According to the method of constructing the relaxation evolution operator (Section 1.1) we consider the modified function $U_M(\lambda, \alpha, r)$:

$$\begin{aligned} &U_M(\lambda, \alpha, r) = U(\lambda, \alpha, r) + \Delta(r) \cdot \frac{\alpha - \alpha_{i+1}}{\alpha_i - \alpha_{i+1}} \cdot \delta(r - r_s), \\ &\alpha \in [\alpha_i; \alpha_{i+1}], \end{aligned} \tag{1.40}$$

such that

$$U_M(\lambda, \alpha_i, r) = U(\lambda, \alpha_i, r) + \Delta(r) \cdot \delta(r - r_s),$$
$$U_M(\lambda, \alpha_{i+1}, r) = U(\lambda, \alpha_{i+1}, r),$$

where $\delta(r)$ is the delta function.

Then the relaxation evolution operator takes the form

$$\hat{L}(\lambda_i, \alpha_i) = L(\lambda_i, \alpha_i) + \frac{\Delta(r_s) \cdot \psi^2(r_s)}{L_\lambda(\lambda_i, \alpha_i) \cdot (\alpha_{i+1} - \alpha_i)}. \quad (1.41)$$

The second term in the right-hand side of (1.41) corresponds to the Newton correction in the OE (1.8).

Thus, the variant of the back substitution method used in MPE consists of the integration of (1.36) from the segment ends $r = 0$ and $r = 1$ to the joint point, r_s, i.e., calculation of the function $D(r)$ in the form (1.38)—direct move—and integration of (1.37) from r_s to the ends of segment $[0; 1]$, i.e., calculation of the eigenfunction $\psi(r)$—back move. Simultaneously we calculate the operators $L_\alpha(\lambda, \alpha)$, $L_\lambda(\lambda, \alpha)$, and the Newton correction, i.e., the relaxation evolution operator $\hat{L}(\lambda_i, \alpha_i)$.

Note that, by definition, the function $D(r)$ is singular and has a discontinuity of the second kind at the zeros of the eigenfunction $\psi(r)$. To calculate $D(r)$ a nonlinear second-order difference scheme was proposed in [20], which takes into account the singularity of this function. It has the form

$$D_{i+1} = \frac{D_i \cdot (h_i^{-1} - 0.5 \cdot U_i \cdot h_i) - 0.5 \cdot (U_i + U_{i+1})}{A_i + \varepsilon \cdot \operatorname{sign} A_i} \cdot$$
$$A_i = D_i + (h_i^{-1} - 0.5 \cdot U_i \cdot h_i). \quad (1.42)$$

In (1.42) $h_i = r_{i+1} - r_i$ $(0 = r_1 < r_2 < \cdots < r_N = 1)$ while ε is chosen empirically. For example, for the 48-digit BESM-6 computer it was chosen as $\varepsilon = 10^{-8}$.

In order to avoid arbitrariness in the choice of ε and to eliminate another source of errors in calculating the function D the following approach has been developed (Fig. 2). The function $W = 1/D$ is introduced and the calculations are made by using the scheme

$$D_{i+1} = F_i^{-1} \cdot [D_i \cdot G_i - 0.5 \cdot (U_i + U_{i+1})], \quad (D)$$

where

$$G_i = h_i^{-1} - 0.5 \cdot U_i \cdot h_i, \qquad F_i = D_i + G_i,$$

if $|D_i|^2 \leqslant 1$, and the scheme

$$W_{i+1} = \frac{1 + G_i \cdot W_i}{G_i - 0.5 \cdot W_i \cdot (U_i + U_{i+1})}, \quad (W)$$

otherwise.

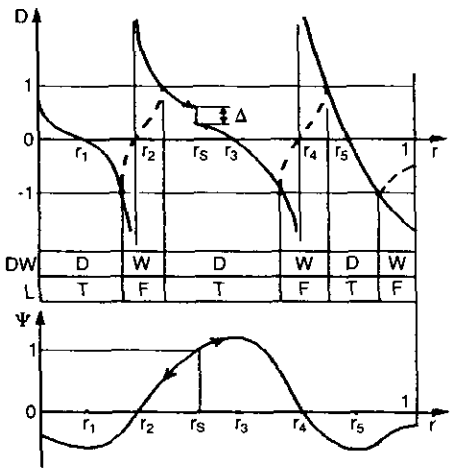

FIG. 2. Calculation arrangement.

The eigenfunction ψ is calculated by back substitution from $r = r_s$ to points $r = 0$ and $r = 1$. Since ψ is determined to within the constant multiplier, at the joint point it is put equal to unity, i.e., $\psi(r_s) = 1$. Further calculations of the eigenfunction are carried out in the following way.

At the back substitution from $r = r_s$ to $r = 0$ we calculate ψ by using the scheme

$$\psi_{i-1} = \psi_i / (h_{i-1} \cdot F_{i-1}),$$

if D_i is determined by the scheme (D), and we use the scheme

$$\psi_{i-1} = (\psi_i \cdot W_{i-1}) / (h_{i-1} \cdot F_{i-1})$$

if D_i is determined by the scheme (W).

At the back substitution from $r = r_s$ to $r = 1$ we calculate ψ by using the scheme

$$\psi_{i+1} = -\psi_i / (h_i \cdot F_{i+1})$$

if D is determined by the scheme (D); otherwise,

$$\psi_{i+1} = -(\psi_i \cdot W_{i+1}) / (h_i \cdot F_{i+1}).$$

The integrals in the operators L_α and L_λ (1.34) are calculated by the trapezoidal method. Thus, to determine the OE the second-order schemes are used in all computations.

Evolution of the eigenvalue of λ with respect to parameter α is determined by the scheme

$$\lambda_{i+1} = \lambda_i + \hat{L}(\lambda_i, \alpha_i) \cdot \delta\alpha_i + O(\delta\alpha_i^2), \quad (1.43)$$

where $\hat{L}(\lambda_i, \alpha_i)$ is described by formula (1.41). According to Section 1.1 the scheme (1.43) is also of second-order accuracy.

Now we shall pass to dimensionless variables, choosing the inner beam radius b_i as the unit length and the cyclotron frequency ω_c as the unit frequency. Let us introduce the designations

$$\xi = r/b_i, \qquad \xi_e = b_e/b_i,$$
$$\zeta_i = a_i/b_i, \qquad \zeta_e = a_e/b_i,$$
$$\Omega = \omega/\omega_c, \qquad \Omega_0 = \omega_0/\omega_c,$$
$$\Omega_s = \omega_s/\omega_c = \Omega - l\cdot\Omega_0, \qquad \Omega_b^2 = \omega_b^2/\omega_c^2,$$

and the focusing parameter,

$$\beta = \omega_i/\omega_c.$$

Then Eq. (3.10) and the boundary conditions (3.11) may be rewritten in the form

$$\frac{1}{\xi}\cdot\frac{d}{d\xi}\left(\xi(\Omega_s^2-\Omega_b^2)\frac{df}{d\xi}\right) - \left(\frac{l^2}{\xi^2}\cdot(\Omega_s^2-\Omega_b^2)+\frac{4\cdot l\cdot\Omega_s\cdot\beta}{\xi^4}\right)\cdot f = 0 \tag{3.12}$$

$$\left(1-\frac{\Omega_b^2}{\Omega_s^2}\right)\cdot\left(\frac{1}{f}\cdot\frac{df}{d\xi}\right)\Bigg|_{\xi=1} = l\cdot\left\{\frac{1+\zeta_i^{2l}}{1-\zeta_i^{2l}}-\frac{2\beta}{\Omega_s}\right\}_{\xi=1}$$
$$\left(1-\frac{\Omega_b^2}{\Omega_s^2}\right)\cdot\left(\frac{1}{f}\cdot\frac{df}{d\xi}\right)\Bigg|_{\xi=\xi_e} = \frac{l}{\xi_e}\cdot\left\{\frac{\xi_e^{2l}+\zeta_e^{2l}}{\xi_e^{2l}-\zeta_e^{2l}}-\frac{2\beta}{\Omega_s\xi_e^2}\right\}_{\xi=\xi_e}. \tag{3.13}$$

Here, in accordance with (3.4)–(3.6),

$$\beta = \pm\left(\frac{1}{4}+2\cdot\frac{e\cdot\kappa_e}{m\cdot b_i^2\cdot\omega_c^2}\right)^{1/2}$$
$$\Omega_0(\xi) = 0.5+\beta/\xi^2, \tag{3.14}$$
$$\Omega_b^2(\xi) = 0.5+2\beta^2/\xi^4, \qquad \Omega_s = \Omega - l\cdot\Omega_0.$$

By using rather simple transformations, the problem (3.12)–(3.13) is reduced to the form (0.1).

For this problem it is sufficiently easy to determine an initial point of the evolution. At $\beta = 0$ the problem can be solved analytically and yields four eigenvalues:

$$\Omega_{1,2,3,4} = \pm 0.5\cdot\{1+g_{1,2}\}^{-1/2},$$
$$g_{1,2} = M\pm[M^2-K_iK_e]^{+1/2},$$
$$M = 0.5\cdot(K_i+K_e)\cdot\frac{(\xi_e^{2l}+1)}{(\xi_e^{2l}-1)},$$
$$K_i = \frac{1+\zeta_i^{2l}}{1-\zeta_i^{2l}}, \qquad K_e = \frac{\xi_e^{2l}+\zeta_e^{2l}}{\xi_e^{2l}-\zeta_e^{2l}}.$$

Thus, the eigenvalue sought in the problem (3.12)–(3.13) is the normalized frequency of the perturbations, $\Omega\in C$, while the physical parameters are the focusing parameter, $\beta\in R$, the azimuthal wave number of perturbation, $l\in Z$, and the geometrical parameters: ζ_i, ζ_e, and ξ_e (the radii of internal and external electrodes, and the external beam radius, respectively; $\zeta_i, \zeta_e, \xi_e\in[0;+\infty)$).

3.1.4. *Numerical Analysis*

The formulated problem was solved by the MPE. For the through-evolution across the bifurcation points (Fig. 5) the prediction algorithm and the Algorithm 2 for evolution curve branching were used. The main purpose of the study was to determine how the stability of the configuration under consideration depends on the focusing parameter β defined by the charge of the internal electrode. From the physical point of view, this parameter causes a shear of the beam angular velocity: when $\beta = 0$ the beam rotates as a solid whole; and as the absolute value of β increases the slippage of electron layers, and hence the relative velocities of the boundary surfaces, grow. As a consequence of the excitation of surface and volume waves, which carry negative energy due to the relative motion of the electron layers and their possible beam interaction, instability may occur [35].

By analogy with plane geometry [32], we should expect two kinds of instability in this problem. The first is caused

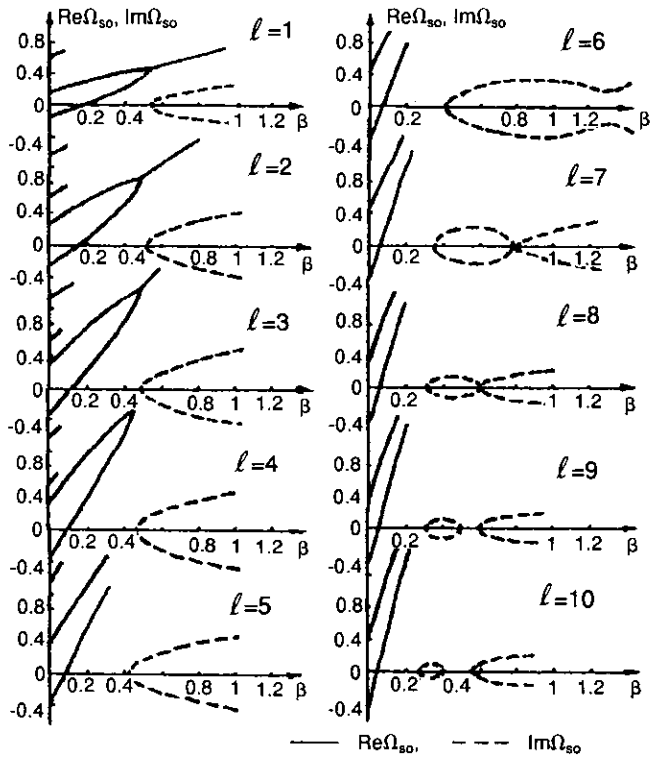

FIG. 5. Curves of $\Omega_{s0}(\beta)$ for $l = 1, \ldots, 10$ with $\zeta_i = 0.1$, $\zeta_e = 2.0$, $\xi_e = 1.2$.

by the interaction of the perturbations at the beam boundaries. This is known as the long wave diocotron instability and may occur only for sufficiently long wave perturbations because short waves on two opposite surfaces of beam get out of resonance, a necessary condition for beam instability.

In the case of cylindrical geometry, the wave length of the azimuthal perturbation cannot exceed the length of the circumference of the beam; the conditions for long wave diocotron instability may be satisfied, if ever, for lower modes only.

The second kind of instability, the gyroresonant or magnetron instability [32, 36], is caused by the interaction of one of the beam surfaces with an internal (resonant) electron layer. In plane geometry [32] this instability occurs for the short wave length only. It should manifest itself in the cylindrical geometry also, since curvature is not essential with decreasing wave length. Thus, a signifcant difference between the cylindrical and plane geometries should be expected for the diocotron instability only, i.e., for large scale perturbations of lower mode type. Therefore, detailed calculations were carried out only for the first 10 modes: $l = 1, 2, ..., 10$.

It is natural to choose the focusing parameter β, representing specific features of cylindrical geometry, as the evolution parameter. The curves $\Omega(\beta)$ constructed for each value of l are, to a certain degree, an analog of dispersion curves because they also contain information about the instability increment depending on the velocity shear. By using these curves we may construct the dispersion function $\Omega(l)$ for each value of β.

By proceeding from the formulation of problem (3.12)–(3.13) we may show that the curves $\Omega_{s0} = \Omega - 0.5 \cdot l$ as a function of β must be asymmetric relative to the axis $\beta = 0$ (odd functions of β) and that the complex-conjugate values must also be solutions. Hence, to determine instability it is sufficient to consider the half-plane $\beta > 0$ only.

The instability increment $\delta = |\mathrm{Im}\, \Omega_{s0}| = |\mathrm{Im}\, \Omega|$ and $\mathrm{Re}\, \Omega_{s0}$ as a function of β are shown in Fig. 5 for values l

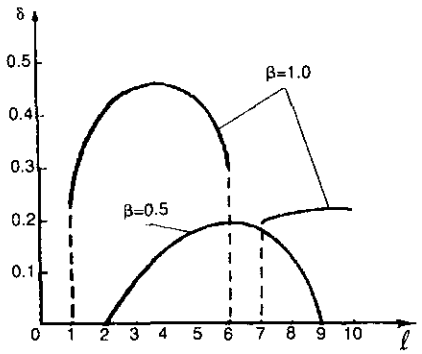

FIG. 6. Increment versus azimuthal wave number.

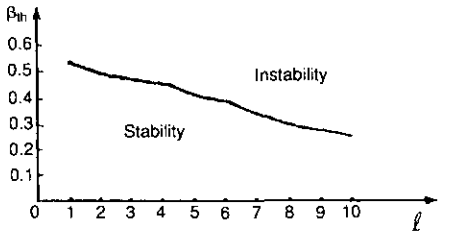

FIG. 7. Threshold value β_{th} required for stabilizing the perturbation depending on azimuthal wave number.

from 1 to 10 for the following geometric parameters: $\zeta_i = 0.1$, $\zeta_e = 2.0$, $\xi_e = 1.2$.

The value $\beta = 0$ corresponds to a negative charge on an internal electrode, equal to the charge required to fill up the space within the tube beam so that it would become a solid Brillouin beam rotating as a whole; in this case there is no velocity shear in the tube beam. The value $\beta = 0.5$ corresponds to zero charge on internal electrode so that the latter may be removed, and the beam becomes hollow. For $l = 1$ there is the stability zone $\beta \in (0; 0.5)$ which monotonically narrows down with growing l. However, even for $l = 10$ it remains finite, $\beta \in (0; 0.26)$. The evolution of curve topology in the instability zone for increasing l is shown in Fig. 5: at $l = 6$ the topology of curves in the β region under consideration begins changing, while for $l > 8$ there appear two zones corresponding to both the diocotron and the gyroresonant instabilities.

By using these curves we construct the dispersion curves $\Omega(l)$ for different β, i.e., for different cases of the beam focusing. The functions $\delta(l)$ for $\beta = 0.5$ and $\beta = 1.0$ are given in Fig. 6. For $\beta = 0.5$ only the long wave diocotron instability may be observed in the considered interval of l, while for $\beta = 1.0$ both instabilities are observed.

For practical purposes the threshold value β_{th} required for stabilizing the perturbation with given azimuthal wave number l is of interest. It is shown in Fig. 7 for the above noted geometry of the beam and the electrodes.

For $\beta > 0.5$ the charge on internal electrode is positive; it corresponds to instability for all l. On the contrary, when $\beta < 0.5$, i.e., for negative charge on internal electrode, sufficiently large scale perturbations may be stabilized.

Thus, it follows from the calculations given that in non-vortex tube beams, like in essentially vortex beams [31], the charge of the internal electrode defines the stability of the beam against lower modes of azimuthal perturbations ($l < 10$).

3.2. Vortex Isorotational Beam

3.2.1. *Introduction*

Isorotational beams of charged particles are cylindrical beams homogeneously rotating with respect to a lon-

gitudinal axis. Such beams may be obtained, for example, by injection from the gun region into the drift region through a jump in the longitudinal magnetic field strength, as in the formation of a Brillouin flow beam [7]. If the density and, hence, current of this beam are below limiting values corresponding to the Bursian–Pavlov instability threshold [35], the only instabilities occurring in it may be caused by a nonhomogeneity of the hydrodynamic velocity field [33]. Since the beam rotation is homogeneous, the diocotron instability due to nonhomogeneity of the transverse velocity component is impossible. Thus, only the instability caused by nonhomogeneous longitudinal velocity, usually called the slipping-instability [37], may occur in such a beam.

However, the slipping-instability of both compensated [37] and noncompensated [38] electron beams have been studied so far only in the case of their strong magnetization, when the drift approximation may be applied and the plasma-to-cyclotron frequency ratio is a small parameter in the problem. Isorotational beams, however, may be formed so that this ratio will exceed unity—it is determined by the value and the sign of the magnetic flux through the emitting surface of the cathode [7].

The main purpose of this section is to study the hydrodynamic stability of isorotational beams without imposing the drift approximation.

The study is carried out within the potential approximation; i.e., the relative velocity field is assumed to be nonrelativistic. Even in this approximation, a resulting equation for the complex amplitude of the helical wave of the potential perturbation with corresponding boundary conditions cannot be fully analysed mathematically by approximate analytical methods [39]. Calculational curves for the basic characteristics of the instability as functions of different parameters were therefore obtained by the MPE. These curves may be used for estimating the transverse dimensions and the critical current of an extended beam.

3.2.2. *Equations Describing the Stationary State*

A general sketch of the axisymmetrical isorotational beam is given in Fig. 8. In cylindrical coordinates (r, φ, z) with the unit vectors $(\mathbf{e}_r, \mathbf{e}_\varphi, \mathbf{e}_z)$, respectively, the z axis coincides with the symmetry axis of the nonperturbed beam. The equations system of one-velocity electron hydrodynamics for nonrelativistic motion of particles in the potential electric field is

$$\begin{aligned} &\partial \mathbf{v}/\partial t + (\mathbf{v}\cdot\operatorname{grad})\mathbf{v} = -(q/m)\cdot\operatorname{grad}\Phi + (q/mc)\cdot[\mathbf{v}\times\mathbf{H}], \\ &\partial n/\partial t + \operatorname{div}(n\cdot\mathbf{v}) = 0, \\ &\nabla^2\Phi = -4\cdot\pi\cdot q\cdot n. \end{aligned} \tag{3.15}$$

Here $\mathbf{v} = (v_r, v_\varphi, v_z)$ is the hydrodynamic velocity vector, $\mathbf{H} = (0, 0, H)$ is the strength vector of the external homogeneous magnetic field, Φ is the electric field potential, n is the electron density, and c is the speed of light (absolute units are used).

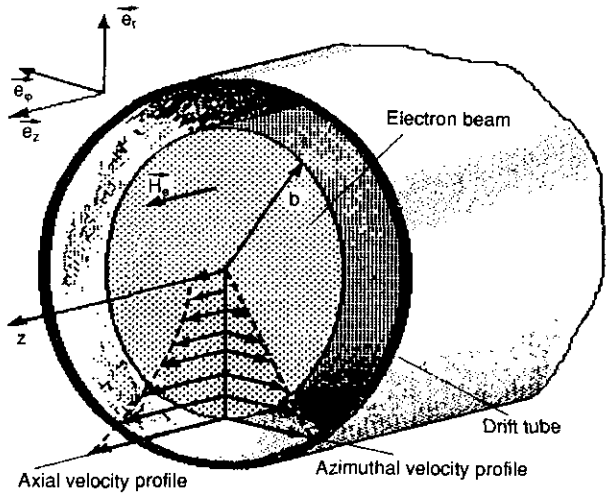

FIG. 8. Isorotational beam.

For axisymmetric beams Bush's theorem is valid [7]; consequently, given that $\partial/\partial t = 0$ and $\partial/\partial\varphi = 0$, the system of equations (3.15) has the motion integral

$$\omega_0(r) = \frac{q}{mc}\cdot\frac{1}{2\pi r^2}\cdot[\psi(r) - \psi_c],$$

where ψ_c is the magnetic flux through a so-called "liquid" circle contour on the cathode surface with the centre on the symmetry axis, which consists of the beam particles and moving with them it becomes of radius r in the beam drift region; $\psi(r)$ is the magnetic flux through the same "liquid" contour in the drift region. Since the magnetic field in the drift region is longitudinal and homogeneous, the angular velocity of the beam rotation is

$$\omega_0 = -0.5\cdot\omega_c\cdot(1 - s), \tag{3.16}$$

where ω_c is the cyclotron frequency, $s \equiv \psi_c/\psi$ is the parameter of the cathode shield against the external magnetic field. Here ψ_c and ψ are the full magnetic fluxes through the beam cross section on the cathode surface and in the drift region, respectively. It is obvious that $\omega_0 = \text{const}$ only when $s = \text{const}$, which is assumed henceforth. This condition can be satisfied, for example, by introducing a beam of constant radius into the drift region through a jump in the longitudinal magnetic field strength, as occurs in Brillouin beam formation [7]. The parameter s may take negative values if the longitudinal magnetic field changes both in value and direction at the jump (reverse focusing).

By substituting the expression (3.16) into the first equa-

tion of system (3.15), which is the equilibrium condition for the stationary beam, we obtain

$$(q/m)\cdot \operatorname{grad} \Phi_0 = -0.25\cdot r\cdot \omega_c^2\cdot(1-s^2). \tag{3.17}$$

Considering conservation of energy, we obtain for an equipotential cathode

$$v_{0z} = \{v_0^2 + 0.5\cdot r^2\cdot\omega_c^2\cdot s\cdot(1-s)\}^{1/2}, \tag{3.18}$$

where v_0 is the beam velocity on the axis. Further, by substituting the expression (3.17) into the Poisson equation we find that

$$\omega_b^2 = 0.5\cdot\omega_c^2\cdot(1-s^2), \tag{3.19}$$

where ω_b is the plasma frequency. From (3.19) it is seen that the parameter s cannot exceed unity in modulus.

Thus, the expressions (3.16)–(3.19) describe the stationary state of the isorotational beam under consideration.

3.2.3. *Formulation of the Spectral Boundary Value Problem*

Now we linearize Eqs. (3.15) near the considered stationary solution describing a nonperturbed beam in the drift tube, all the parameters of which depend on r only. To do this we present the functions in the equations as a sum of their nonperturbed values and perturbations:

$$\begin{aligned} \mathbf{v} &= \mathbf{v}_0(r) + \mathbf{v}_1(r,\varphi,z,t),\\ \Phi &= \Phi_0^{(r)} + \Phi_1(r,\varphi,z,t),\\ n &= n_0(r) + n_1(r,\varphi,z,t), \end{aligned} \tag{3.20}$$

where the lower indices 0 and 1 refer, respectively, to the nonperturbed values and perturbations.

The desired perturbations may be presented in the form of helical harmonics of the normal wave, i.e.,

$$a_1(r,\varphi,z,t) = \tilde{a}(r)\cdot\exp\{-i\cdot(\omega t - l\varphi - k_z z)\}, \tag{3.21}$$

where $\tilde{a}(r)$ is a complex amplitude of the helical wave of perturbation of respective quantity, ω is the wave frequency, l and k_z are, respectively, azimuthal and axial wave numbers.

By substituting the expressions (3.20) into (3.15), linearizing the latter with respect to the perturbations and presenting the perturbations in the form (3.21), we express the amplitude $\tilde{a}(r)$ of all desired parameters in terms of the amplitude of the potential (to simplify the writing we further omit the tilde above the quantities). Thus we obtain

$$v_r = i\cdot\frac{q}{m}\cdot\left(\frac{\omega_{vz}}{\omega_s^2-\omega_{vz}^2}\cdot\frac{l}{r}\cdot\Phi - \frac{\omega_s}{\omega_s^2-\omega_{vz}^2}\cdot\frac{d\Phi}{dr}\right),$$

$$v_\varphi = \frac{q}{m}\cdot\left(\frac{\omega_s}{\omega_s^2-\omega_{vz}^2}\cdot\frac{l}{r}\cdot\Phi - \frac{\omega_{vz}}{\omega_s^2-\omega_{vz}^2}\cdot\frac{d\Phi}{dr}\right),$$

$$v_z = \frac{q}{m}\cdot\left(\frac{k_z}{\omega_s}\cdot\Phi - \frac{\omega_{v\varphi}}{\omega_s}\cdot\frac{\omega_{vz}}{\omega_s^2-\omega_{vz}^2}\cdot\frac{l}{r}\cdot\Phi + \frac{\omega_{v\varphi}}{\omega_s^2-\omega_{vz}^2}\cdot\frac{d\Phi}{dr}\right),$$

$$\begin{aligned} n = n_0\cdot\frac{q}{m}\cdot\Bigg\{&\frac{1}{r}\cdot\frac{d}{dr}\left(r\cdot\frac{1}{\omega_s^2-\omega_{vz}^2}\cdot\frac{d\Phi}{dr}\right)\\ &-\left(\frac{1}{\omega_s^2-\omega_{vz}^2}\cdot\frac{l^2}{r^2}+\frac{k_z^2}{\omega_s^2}\right.\\ &\left.-k_z\cdot\frac{l}{r}\cdot\frac{\omega_{v\varphi}\omega_{vz}}{\omega_s^2(\omega_s^2-\omega_{vz}^2)}-\frac{l}{r\omega_s}\cdot\frac{d}{dr}\frac{\omega_{vz}}{\omega_s^2-\omega_{vz}^2}\right)\Phi\Bigg\}. \end{aligned}$$

Here we have following nomenclature:

$\omega_s = \omega - l\omega_0 - k_z\cdot v_{0z}$ is the Doppler shift frequency;

$\boldsymbol{\omega}_c = (q/mc)\cdot\mathbf{H}$ is the cyclotron frequency vector;

$\boldsymbol{\omega}_v = \boldsymbol{\omega}_c + \operatorname{curl}\mathbf{v}_0$ is the vortex vector.

By substituting the expression for the beam density amplitude into the Poisson equation (the third equation in the system (3.15)) we reduce the linearized system to a single equation for the complex amplitude of the helical wave of perturbation. As a result, we have

$$\begin{aligned} &\frac{1}{r}\cdot\frac{d}{dr}\left[r\cdot\left(1-\frac{\omega_b^2}{\omega_s^2-\omega_{vz}^2}\right)\cdot\frac{d\Phi}{dr}\right]\\ &\quad-\left\{\left(1-\frac{\omega_b^2}{\omega_s^2-\omega_{vz}^2}\right)\cdot\frac{l^2}{r^2}\right.\\ &\quad+\left(1-\frac{\omega_b^2}{\omega_s^2}\right)\cdot k_z^2 + k_z\cdot\frac{l}{r}\cdot\frac{\omega_{v\varphi}\omega_{vz}\omega_b^2}{\omega_s^2(\omega_s^2-\omega_{vz}^2)}\\ &\quad\left.+\frac{l}{r}\cdot\frac{\omega_b^2}{\omega_s}\cdot\frac{d}{dr}\frac{\omega_{vz}}{\omega_s^2-\omega_{vz}^2}\right\}\Phi = 0. \end{aligned} \tag{3.22}$$

The requirements that the desired solution be zero at the beam boundary, $r=b$ (Fig. 8) and finite on the beam axis, $r=0$, i.e.,

$$\Phi(0) = \Phi(b) = 0, \tag{3.23}$$

are chosen as the boundary conditions. They correspond to the case when the gap between the beam surface and the drift tube is negligibly small as compared with all other dimensions.

3.2.4. *Numerical Analysis*

Let us introduce the following designations:

$$\xi = r/b; \qquad \lambda = \omega/\omega_c; \qquad \beta = k_z\cdot b; \qquad v = [v_0/(\omega_c\cdot b)]^2.$$

Then the spectral boundary value problem (3.22)–(3.23) in dimensionless variables may be presented in the form:

$$\frac{1}{\xi}\cdot\frac{d}{d\xi}\left[\xi\cdot\left(1-\frac{\alpha_b^2}{\alpha_s^2-s^2}\right)\cdot\frac{d\Phi}{d\xi}\right] - \left\{\left(1-\frac{\alpha_b^2}{\alpha_s^2-s^2}\right)\cdot\frac{l^2}{\xi^2}+\left(1-\frac{\alpha_b^2}{\alpha_s^2}\right)\cdot\beta^2 + \beta\cdot\frac{l}{\xi}\cdot\frac{s\alpha_v\alpha_b^2(3\alpha_s^2-s^2)}{\alpha_s^2(\alpha_s^2-s^2)^2}\right\}\Phi=0, \qquad (3.24)$$

$$\Phi(0)=\Phi(1)=0,$$

where

$$\alpha_b^2=0.5\cdot(1-s^2),$$

$$\alpha_s=\lambda-0.5\cdot l\cdot(1-s)-\beta\cdot(v+0.5\cdot\xi^2 s(1-s))^{1/2},$$

$$\alpha_v=\frac{\xi\cdot s\cdot(1-s)}{2\cdot(v+0.5\cdot\xi^2 s(1-s))^{1/2}},$$

$$l=1,2,3,\ldots, \qquad \beta\in(+\infty;-\infty),$$

$$s\in[0;1], \qquad v\in[0;+\infty).$$

The formulated spectral boundary value problem can be investigated thoroughly by using numerical methods. Such an investigation was carried out by the MPE. Now we discuss the physical results obtained.

The purpose of calculations was to obtain curves for basic instability characteristics depending on parameters that determine the initial beam equilibrium or the type of perturbation.

In Figs. 9 and 10 the dimensionless increment of instability, $\delta=|\mathrm{Im}\,\lambda|$, and the real part of the frequency, Re λ, are shown, respectively, versus the longitudinal wave number β for $s=0.5$, $v=1.0$, and eight values of azimuthal wave number $l=1, 2, \ldots, 8$. For all l the increment reaches a maximum in the region of β-values corresponding to instability. Although the curves are nonsymmetric, their maxima are located approximately in the middle of the instability region, which corresponds to qualitative picture of most vigorously growing perturbations.

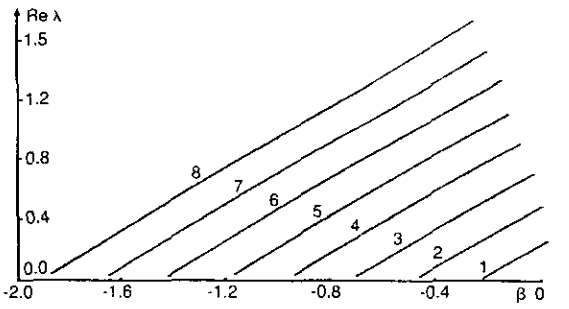

FIG. 10. Real part of frequency depending on axial wave number: $s=0.5$; $v=1.0$; $l=1, \ldots, 8$.

The instability increment δ depending on the cathode shielding parameter s in the interval $(0; 1)$ for $v=1.0$ and wave number $\beta=0.5\cdot\beta^*$, where $\beta^*=0.5\cdot l\cdot(1-s)/(v+0.125\cdot s(1-s))^{1/2}$, is given in Fig. 11 for different $l=1, \ldots, 8$. From this figure it is seen that the increment reduces to zero at the ends of this interval and reaches a maximum approximately in its middle, which corresponds to the magnetic field strength $\approx 1.2\cdot H_{\min}$, where $H_{\min}$ is the least magnetic field strength, which is necessary for the confinement of an electron beam of required density (Brillouin value). Thus, at the formation of stable beams similar to the ones under consideration we should choose the magnetic fields whose values are at least two times greater than the Brillouin value, as is usually done in practice.

Figure 12 shows the real part of frequency Re λ versus the parameter s for the same values of all the other parameters.

For each value of azimuthal wave number l there is an infinite number of higher order modes corresponding to the roots μ_{ln} of the lth-order Bessel functions with growing n. The higher modes are given in Figs. 13–16 for several initial values of n. The dispersion curves $\delta(\beta)$ and Re $\lambda(\beta)$ are given, respectively, in Figs. 13 and 14 for $s=0.5$ and $v=1.0$ while $l=1$ and $n=1, 2, 3, 4$. It may be seen that for each mode the behavior of the curve is approximately the same;

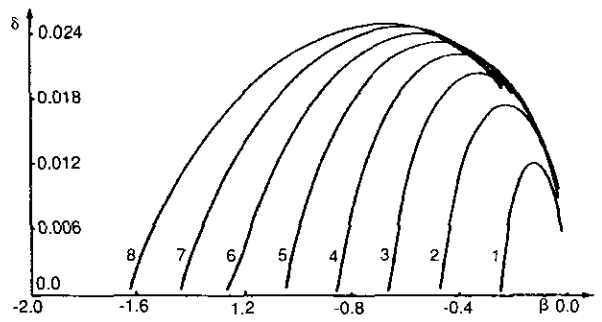

FIG. 9. Instability increment depending on axial wave number: $s=0.5$; $v=1.0$; $l=1, \ldots, 8$.

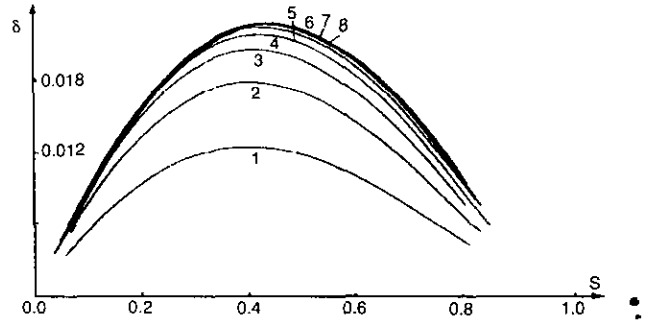

FIG. 11. Instability increment depending on cathode shielding parameter: $\beta=0.5\cdot\beta^*$; $v=1.0$; $l=1, \ldots, 8$.

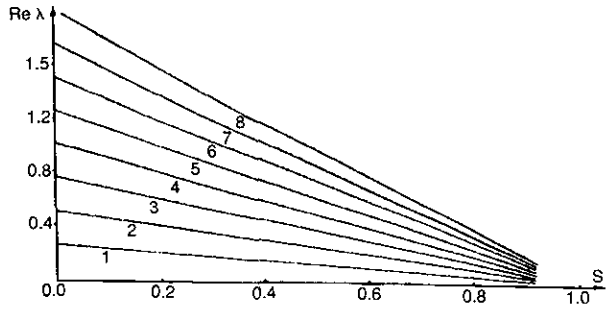

FIG. 12. Real part of frequency depending on cathode shielding parameter: $\beta = 0.5 \cdot \beta^*$; $v = 1.0$; $l = 1, ..., 8$.

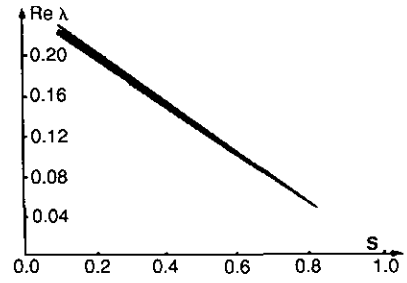

FIG. 16. Curves of Re $\lambda(s)$ for higher modes: $\beta = 0.5 \cdot \beta^*$; $v = 1.0$; $l = 1$; $n = 1, 2, 3, 4$.

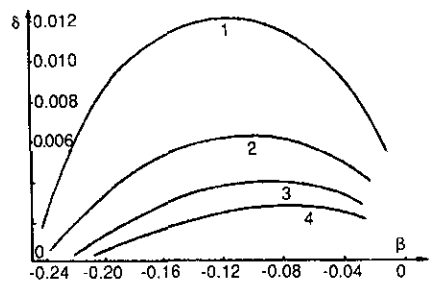

FIG. 13. Curves of $\delta(\beta)$ for higher modes: $s = 0.5$; $v = 1.0$; $l = 1$; $n = 1, 2, 3, 4$.

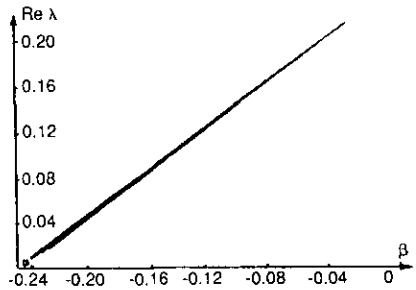

FIG. 14. Curves of Re $\lambda(\beta)$ for higher modes: $s = 0.5$; $v = 1.0$; $l = 1$; $n = 1, 2, 3, 4$.

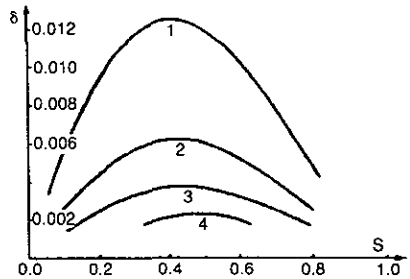

FIG. 15. Higher mode increments versus parameter s: $\beta = 0.5 \cdot \beta^*$; $v = 1.0$; $l = 1$; $n = 1, 2, 3, 4$.

if the curves Re $\lambda(\beta)$ nearly coincide, the increment values decrease with growing n. In this manner, the lower mode will be the most dangerous among those considered. The same conclusion follows from an analysis of the curves for the same values given in Figs. 15 and 16, depending on the parameter s at $\beta = 0.5 \cdot \beta^*$, $v = 1.0$ for $l = 1$ and $n = 1, 2, 3, 4$.

Figures 17 and 18 show the increment δ and the real part of the frequency versus parameter v at $s = 0.5$ and $\beta = 0.5 \cdot \beta^*$ for $l = 1, ..., 8$ and $n = 1$. As a growth of v is equivalent to a decrease in the beam perveance and density, it is natural that a reduction in the increment for all l is observed (Fig. 17). The real part of the frequency seems to decrease due to diminishing angular velocity.

Thus, instability of noncompensated beams of charged particles due to nonhomogeneity of longitudinal velocity (slipping instability) has been studied first without imposing the drift approximation constraints, i.e., for any degree of cathode shielding against the external magnetic field.

The obtained quantitative dependences of basic instability characteristics on the beam parameters and the perturbation are of practical interest and may be used in the design calculations and assessments.

It is usual that in practice the magnetic field used for beam maintenance in the drift tube is chosen approximately

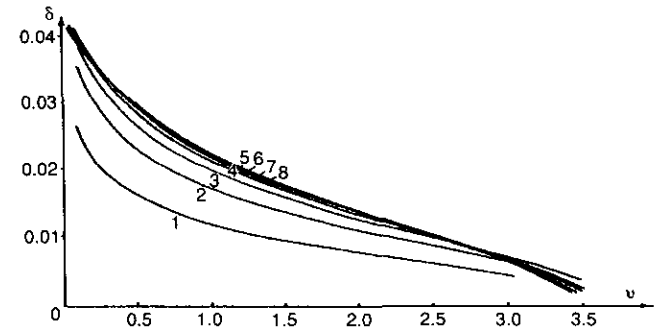

FIG. 17. Instability increment depending on parameter v: $\beta = 0.5 \cdot \beta^*$; $s = 0.5$; $l = 1, ..., 8$.

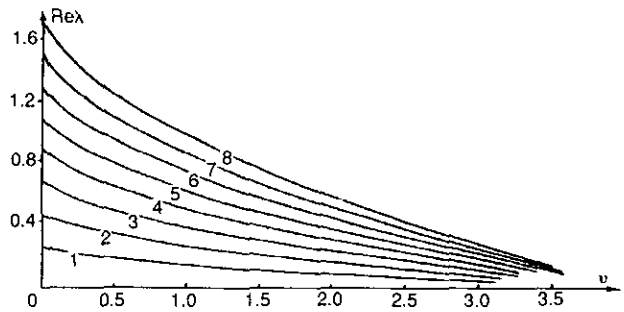

FIG. 18. Curves of Re $\lambda(v)$: $\beta = 0.5 \cdot \beta^*$; $s = 0.5$; $l = 1, \ldots, 8$.

equal to double the Brillouin field. According to this analysis, such an empirical choice is quite reasonable because it corresponds to the stable state of the beam.

REFERENCES

1. M. L. Andrews, H. Davitian, H. H. Fleischmann, R. E. Kribel, V. R. Cusse, J. A. Nation, R. Lee, R. V. Lovelace, and R. N. Sudan, "Application of Intense Relativistic Electron Beams to Astron-Type Experiments," *Plasma Physics and Controlled Nuclear Fusion Research.* (International Atomic Energy Agency, Vienna, 1971), Vol. 1, 169.
2. V. I. Vexler, in *Proceedings, CERN Symp. on High-Energy Accelerations and Pion Physics.* (CERN Scientific Information Service, Geneva, 1956), Vol. 1, 80.
3. A. N. Didenko, V. P. Grigorjev, and Yu. P. Usov, *Powerful Electron Beams and Their Application* (Atomizdat, Moscow, 1977).
4. P. T. Kirstein, G. S. Kino, and W. E. Waters, *Space-Charge Flow.* (McGraw-Hill Book, New York, 1967).
5. V. G. Leyman, *Radiotekhn. i Electron.* **25** (2), 2410 (1980).
6. N. A. Kroll and A. W. Trivelpiece, *Principles of Plasma Physics* (McGraw-Hill, New York, 1973).
7. J. D. Lawson, *The Physics of Charged-Particle Beams*, (Clarendon Press, Oxford, 1970).
8. R. F. Davidson, *Theory of Nonneutral Plasmas* (Benjamin-Cummings, Menlo Park, CA, 1974).
9. N. N. Kalitkin, *Numerical Methods* (Nauka, Moscow, 1978).
10. I. D. Rodionov, Preprint 23; Keldysh Inst. Appl. Math., USSR Acad. Sci., 1982.
11. L. V. Kuzmina and I. D. Rodionov, Solving systems of the Hartree-equations by the method of parameter evolution. *Zh. vychisl. Mat. i Mat. Fiz.* **25** (8), 1200 (1985).
12. I. D. Rodionov, Ph.D. thesis (UINR, Dubna, 1988).
13. H. Wacker (Ed.), *Continuation Methods. Proceedings, Symposium at the University of Lins, Austria, October 3–7, 1977* (Academic Press, New York, 1978).
14. J. M. Ortega and W. C. Rheinboldt, *Iterative Solution of Nonlinear Equations in Several Variables* (Academic Press, New York/London, 1970).
15. H. Schwetlick, Ein neues princip der konstruktion implementer-barer, global konvergenter Einbettungs-algorithmen (test beispiele). *Beitr. Numer. Math.* **5**, 201 (1976).
16. S. P. Litvintseva and I. D. Rodionov, Preprint 75, Keldysh Inst. Appl. Math., USSR Acad. Sci., 1986.
17. S. P. Litvintseva, I. D. Rodionov, and E. B. Solomatin, *Mat. Model.* 1 (12), 52 (1989).
18. T. Y. Na, *Computational Methods in Engineering Boundary Value Problems* (Academic Press, New York, 1979).
19. A. A. Samarskii, *Theory of Difference Schemes* (Nauka, Moscow, 1983).
20. I. D. Rodionov, Calculation of quantum-mechanical scattering by the method of an isolated region. *Zh. Vychisl. Mat. i Mat. Fiz.* **17** (2), 1494 (1977).
21. M. G. Crandall and P. H. Rabinowitz, "Mathematical Theory of Bifurcation," in *Bifurcation Phenomena in Mathematical Physics and Related Topics. Proceedings, NATO Advanced Study Inst.* (Reidel, Dordrecht, 1979), 3.
22. C. Bolley, in *Lect. Notes in Math.*, Vol. 782 (Springer-Verlag, New York/Berlin, 1980), 42.
23. F. Conrad "Approximation of Nonlinear Eigenvalue Problems Associated with Elliptic Variational Inequalities by Continuation Methods," in *Innovative Numerical Methods in Engineering* (Springer-Verlag, New York, 1986), 145.
24. S. B. Margolis, and B. J. Matkowsky, *SIAM J. Appl. Math.* **45** (1) 93 (1985).
25. S. P. Litvintseva and I. D. Rodionov, Preprint 40, Keldysh Inst. Appl. Math., USSR Acad. Sci., 1988.
26. M. Kubicek and A. Klik, *Appl. Math. Comput.* **13** (1–2), 125 (1983).
27. D. W. Decker and H. B. Keller, *Commun. Pure Appl. Math.* **34** (2), 149 (1981).
28. G. Iooss and D. D. Joseph, *Elementary Stability and Bifurcation Theory* (Springer-Verlag, New York, 1980).
29. H. Pötzl, *Arch. Electrisch. Ubertragung.* **19** (7) 367 (1965).
30. G. G. MacFarlane and H. G. Hay, *Proc. Phys. B* **63**, 407 (1950).
31. R. H. Levy, *Phys. Fluids*, **8** (7), 1288 (1965).
32. O. Buneman, R. H. Levy, and L. M. Linson, *J. Appl. Phys.* **37**, 3203 (1966).
33. A. D. Gladun and V. G. Leyman, *Zh. Tekhn. Fiz.* **11** (12), 2513 (1970).
34. V. G. Leyman, S. P. Litvintseva, O. B. Ovsyannikova, and I. D. Rodionov, Preprint 115, Keldysh Inst. Appl. Math., USSR Acad. Sci., 1985.
35. M. V. Nezlin, *Beam Dynamics in a Plasma* (Energoizdat, Moscow, 1982).
36. I. Swegle and E. Ott, *Phys. Fluids* **24** (10), 1821 (1981).
37. A. B. Mikhailovsky and A. A. Rukhadze, *Zh. Tekhn. Fiz.* **35** (12), 2143 (1965).
38. J. A. Rome and R. J. Briggs, *Phys. Fluids* **158** (5), 796 (1972).
39. V. G. Leyman, S. P. Litvintseva, O. B. Ovsyannikova, and I. D. Rodionov, Preprint 145, Keldysh Inst. Appl. Math., USSR Acad. Sci., 1987.